Energy analysis of dedicated and integrated mechanical subcooled CO2 boosters for supermarket applications

Article *in* International Journal of Refrigeration · May 2019

DOI: 10.1016/j.ijrefrig.2019.01.034

CITATIONS
0

READS
70

5 authors, including:

Jesús Catalán Gil
Universitat Jaume I
34 PUBLICATIONS **139** CITATIONS
SEE PROFILE

Rodrigo Llopis Doménech
Universitat Jaume I
109 PUBLICATIONS **922** CITATIONS
SEE PROFILE

Daniel Sánchez
Universitat Jaume I
91 PUBLICATIONS **772** CITATIONS
SEE PROFILE

Laura Nebot Andres
Universitat Jaume I
34 PUBLICATIONS **126** CITATIONS
SEE PROFILE

Energy analysis of dedicated and integrated mechanical subcooled CO_2 boosters for supermarket applications.

Jesús Catalán-Gil, Rodrigo Llopis [IIR,*], Daniel Sánchez [IIR], Laura Nebot-Andrés [IIR], Ramón Cabello

Thermal Engineering Group, Mechanical Engineering and Construction Department,

Jaume I University, Spain

*Corresponding author: rllopis@uji.es, +34 964 718136

Abstract

Energy improvements offered by dedicated and integrated mechanical subcooling systems in CO_2 booster systems for supermarket applications are analysed here through the use of thermodynamic models close to reality. Using a reference supermarket with 41kW and 140kW thermal loads at low and medium temperature, respectively, and considering as state-of-the-art system the CO_2 booster with parallel compressor and flash gas by-pass, it has been concluded that both systems allow to reduce energy consumption. However, its operation is highly dependent on environmental conditions. The dedicated mechanical subcooling system offers annual energy reductions for tempered places from 1.5 to 2.9%, for warm between 2.9 to 3.4% and for hot from 3.0 to 5.1%. The integrated subcooling system obtains reductions between 3.1 to 4.0% for cold regions, from 1.4 to 2.9% for tempered, from 2.9 to 3.4% for warm and from 1.3 to 2.4% for hot regions.

Keywords

CO_2; subcooling; dedicated mechanical subcooling; integrated mechanical subcooling; supermarket

IIR: Member of International Institute of Refrigeration, Commission B2.

Nomenclature

BP	back-pressure
CON	condenser
COP	coefficient of performance
CR	compression ratio
D	days of month
DMS	booster with R-290 dedicated mechanical subcooling
DSH	desuperheater
E	energy consumption, kWh
FG	flash gas by-pass valve
HP	high pressure
IHX	internal heat exchanger at low temperature
IMS	booster with integrated mechanical subcooling
LF	load factor
LP	low pressure
LT	low temperature
MT	medium temperature
p	pressure, bar
PC	booster with parallel compression and flash gas by-pass
P_C	compressor power consumption, kW
$\dot{Q}_O$	cooling capacity, thermal load, kW
SUB	subcooler
t	temperature, ºC

Greek symbols

Δ	increment
η_V	compressor's volumetric efficiency
η_G	compressor's overall efficiency
v	specific suction volume, $m^3 \cdot kg^{-1}$
ε	thermal effectiveness

Subscripts

C	compressor rack
dis	discharge
env	environment temperature
K	condenser
MS	refers to the DMS cycle
O	evaporation level
suc	suction
ves	plant vessel

1. Introduction

Revolution of CO_2-based refrigeration systems for supermarkets was initiated by researchers and companies mainly placed in Europe in the last two decades. Their real field-implementation started in the north of Europe due to their favourable environmental conditions, but their enforcement was accelerated by the entry into force of the F-Gas Regulation in 2014 (European Commission, 2014), they now being a reality trough all regions of Europe. However, the operating region extension of CO_2 systems to mild and warm countries was only possible due to the increase in complexity of the systems in relation to the HFC-based ones. Gullo et al. (2018a) reviews the most recent CO_2 refrigeration systems up to the moment and their evolution during the last two decades. Kigali Amendment to the Montreal Protocol, ratified by 53 countries now (September 2018), aims to reduce 70 billion tones $CO_{2,equ}$ by 2020 by phasing-out 85% of HFC gases by late 2040s. Thus, the implementation of CO_2-based supermarket refrigeration systems will be favoured by this agreement worldwide. Therefore, all the changes lived in Europe will be translated to other regions of the World.

CO_2 basic booster system with gas by-pass valve, is the commonly chosen solution for cold and tempered regions, where it has been verified that it overcomes traditional HFC-based systems, being the energy benefit larger if heat recovery is implemented in the system, as evaluated by Sawalha (2013) and measured by Sawalha et al. (2017). They concluded that this system has higher COP than HFC-based systems for outdoor temperatures lower than 24ºC. Considering annual operation, it was able to reduce 11% the electricity consumption in relation to HFC-based systems in the North of Europe (Karampour and Sawalha, 2017). However, the extension of CO_2-based systems to warm and hot regions needs to rely on more complex and advanced systems that compete with traditional supermarket architectures. These new generations of refrigeration systems can be grouped into three big groups: The first one, which relies on the use of auxiliary compressors (parallel compression and integrated mechanical subcooling); the second one, which relies on the use of ejectors or multi-ejector blocks; and the last one, which is based on the thermal interaction of the CO_2 cycle with and additional cycle (cascades, cascaded booster systems or dedicated mechanical subcooling systems).

The first systems group is represented by boosters with parallel compression or auxiliary compression economization. Auxiliary compressors extract vapour from the vessel and compress it to the high pressure, thus reducing vessel pressure, reducing the vapour title at the inlet of the evaporators and shortening the refrigerant mass flow through the high-pressure compressor rack. These systems have been analysed theoretically by Gullo and Hafner A. (2017), Karampour and Sawalha (2018), and others. They perform with higher efficiency than HFC-based systems up to outdoor temperatures of 27ºC (Gullo et al., 2018a). Inside this group, the booster system with integrated mechanical subcooler can be also considered (Llopis et al., 2018). It is based on the use of an additional CO_2 compressor which compresses the refrigerant used to provide subcooling at the exit of the gas-cooler through an additional heat exchanger, allowing to shorten the optimum high pressure of the system and also to reduce the vapour title at the inlet of the evaporators. This architecture, analysed in detail in the present work, has received little attention, since only the theoretical analysis of Cecchinato et al. (2009) and Gullo and Cortella (2016) for single-stage cycles have been found by authors. In contrast to the parallel compression system, the advantage of this configuration is that the pressure lift of the auxiliary compressor is shortened in relation to the parallel configuration (suction pressure higher than vessel pressure and reduced high pressure due to subcooling). Gullo and Cortella (2016) evaluated it theoretically for a single-stage cycle evaporating at -10ºC and outdoor temperature from 30 to 42ºC, and quantified the COP improvement in relation to a parallel compression system between 2.8 to 5.5%. However, this advanced architecture has not been applied to booster systems to the best of the authors' knowledge.

The second group corresponds to booster configuration which use ejectors or multi-ejector blocks (vapour and liquid ejectors) to recover energy in the expansion process at the exit of the gas-cooler. Vapour ejectors are used to pre-compress a part of the refrigerant from the medium pressure level, thus increasing the

suction pressure of parallel compressors, and liquid ejectors are used to increase MT evaporating temperature and pressure level through the use of overfeed evaporators. This group, which is extensively covered in the review of Gullo et al. (2018a) can provide an annual performance energy increase of 15% (Girotto, 2017). Also, this technology has been applied in real supermarkets, where it has been measured that its energy consumption is shortened by 14% in relation to refrigeration systems with parallel compression (Gullo et al., 2018a). According to Gullo et al. (2018b) this technology, with integration of the AC demand, can outperform any solution for supermarket systems at outdoor temperatures even from -10 to 5ºC, with estimation of energy savings and environmental impact reductions of 26.9% and 90.9%. Thus, this technology is able to cover any climate condition.

Finally, the last group of technologies for supermarkets are those based on the use of auxiliary cycles coupled thermally with a main CO_2 cycle. CO_2 with dedicated mechanical subcooling (DMS) was contrasted to cascades for medium temperature applications by Nebot-Andrés et al. (2017), concluding that DMS gets over cascade systems for temperature lifts below 28.5K, and considering annual operation its yearly-performance is better than cascades for evaporating levels higher than -15ºC. However, this system was not evaluated considering a booster solution. Dai et al. (2018) evaluated the CO_2 system with DMS using zeotropic mixtures in the auxiliary cycle. They stated that higher benefits can be obtained with the mixtures than with the use of pure refrigerants and also evaluated their integration by using a thermoelectric subcooler and an expander (Dai et al., 2017). Purohit et al. (2017) presented a theoretical comparison of a R-290 DMS booster solution in contrast to a R-744 booster with parallel compression, concluding that the DMS system only surpasses the only-CO_2 system at very hot climatic conditions, with reductions in annual energy consumption by 6.4 to 8.9%. Other hybrid systems found in literature are the subcritical or cascaded booster systems (Catalán-Gil et al., 2018) and cascades with AC integration (Purohit et al., 2018), which are reliable technologies especially for very hot climatic conditions.

According to the literature, it has been found that CO_2 booster system with integrated mechanical subcooling has not been evaluated for supermarket purposes yet to the best of the authors' knowledge. This system, whose operation relies on the use of an additional compressor and an additional heat exchanger (subcooler) presents some energy advantages in relation to the state-of-the-art booster system which must be highlighted. Therefore, this work is devoted to evaluate the energy performance of this system in relation to the CO_2 booster system with parallel compression (representing the reference system for tempered and cold regions) and to the CO_2 booster system with R-290 DMS (representing a suitable system for warm and hot regions), aiming to clarify the most suitable regions for each system and their pros and cons. The work, developed using close-to-reality models based on compressor manufacturer's data, considers the typical European supermarket as reference ($\dot{Q}_{O,MT} = 140kW$ at -6ºC and $\dot{Q}_{O,LT} = 41kW$ at -32ºC) and avoids to introduce additional measures to improve the overall efficiency, such as flooded evaporators, heat recovery, AC integration or even evaporative cooling, with the intention to clarify systems' understanding. The architectures are evaluated for a wide range of outdoor temperatures (0 to 40ºC), and then, their yearly annual operation is evaluated for 282 locations in Europe and 395 cities of Asia, covering from cold to very hot regions, where their energy improvements and operating parameters are quantified and discussed.

2. Cycles and model assumptions

This section presents the architectures for supermarket applications considered in this work. The systems provide service simultaneously to MT level and LT levels. Section 2.1 describes the common and special characteristics of each refrigeration solution, Section 2.2 details the expressions used to evaluate compressor's performance and Section 2.3 details the boundary conditions and assumptions considered for the energy evaluation of the systems.

2.1. Refrigeration cycles

Refrigeration architectures considered in this work are: a CO_2 refrigeration booster with parallel compression and by-pass gas valve (Figure 1) denoted as PC system; a CO_2 booster with integrated mechanical subcooling (Figure 2) called IMS system; and a CO_2 booster with an R-290 dedicated mechanical subcooling cycle, known as DMS system. The three systems provide simultaneous service to different MT and LT multiplexed systems using direct expansion systems with dry evaporation. All incorporate an air cooled gas-cooler/condenser at the discharge of the high-pressure rack and a low temperature gas-cooler or desuperheater (DSH) at the discharge of the low-pressure rack to release heat to the environment, which enhances the energy performance of the cycle (Karampour and Sawalha, 2018). The DSH is not commonly considered in these cycles because of the increased cost, however, our simulations indicate that the COP improvement due to the DSH in terms of COP ranges between 2.1 to 7.3%, its performance being better at lower environment temperatures. Also, they incorporate an internal heat exchanger (IHX) at the exit of the liquid receiver to guarantee subcooled liquid at the inlet of the expansion devices. This IHX improves the energy performance of subcritical systems (Llopis et al., 2015). In addition, the three architectures operate with a double-stage expansion system, the first stage is devoted to regulate the heat rejection pressure through a back-pressure (BP) and the second to control the evaporation in the services with thermostatic expansion valves.

PC system, whose scheme and pressure-enthalpy is detailed in Figure 1, in addition to the common characteristics described above, incorporates a compressor rack which extracts saturated vapour (point 13, Figure 1) and compresses it to the inlet of the gas-cooler/condenser (point 14, Figure 1). The PC rack decreases pressure in the vessel, increasing the specific cooling capacity and reducing the refrigerant mass flow rate through the LP_C and HP_C racks. It also incorporates a flash-gas by pass valve (FG) which extracts vapour from the vessel at low outdoor temperatures when the PC rack cannot operate due to reduced compression ratio (see Table 2), and injects it at HP_C rack suction.

IMS system, which scheme and pressure-enthalpy diagram are detailed in Figure 2, has the following features: it incorporates a heat exchanger at the exit of the gas-cooler/condenser, called subcooler (SUB). In the SUB, the main refrigerant flow (points 7 to 8, Figure 2) is cooled by heat transfer with an auxiliary flow (points 7, 13 and 14, Figure 2), which is expanded and evaporated in the SUB. Then, the auxiliary flow is recompressed to the high pressure by the IMS_C rack (points 14 to 15, Figure 2). The expansion device regulates the evaporating process (dry evaporation) in the SUB and the degree of subcooling in the heat exchanger is maintained by speed variation of the IMS_C rack, being its reference variable the outlet temperature of the subcooler. The optimum subcooling degree has been evaluated by simulation (Figure 5), thus, for its real implementation the control algorithm of the IMS_C rack drive should be developed. Also, at low outdoor temperatures the subcooling system operates, but the evaporated refrigerant is injected via expansion to the HP_C rack suction (see Table 3).

DMS system (Figure 3) has also a subcooler at the exit of the gas-cooler/condenser to cool CO_2 high-pressure line (points 6 to 7, Figure 3), but in this case the capacity is provided using a single-stage cycle working with R-290 as refrigerant. The degree of subcooling is controlled by speed variation of the DMS_C rack, being its reference variable the outlet temperature of the subcooler as in the IMS system. The DMS auxiliary cycle contains an additional condenser ($COND_{MS}$) and an expansion device that controls the evaporating process of R-290 in the subcooler. This architecture does not include the flash-gas by pass

valve because its energy efficiency is lower than with the considered configuration. Also, this configuration does not include the parallel compressor to avoid increased cost of the system.

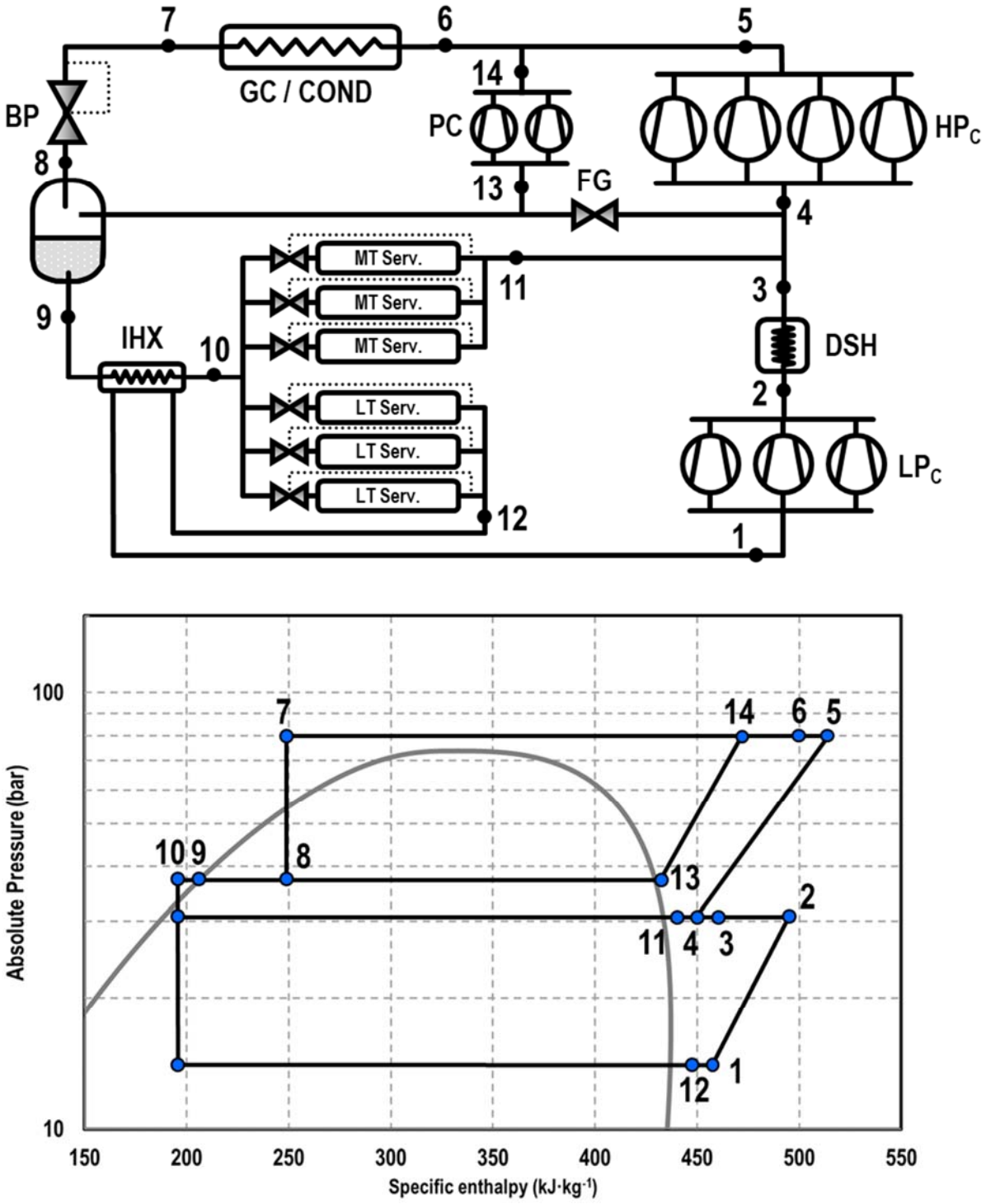

Figure 1. Schematic diagram and Ph diagram of refrigeration booster with parallel compressor

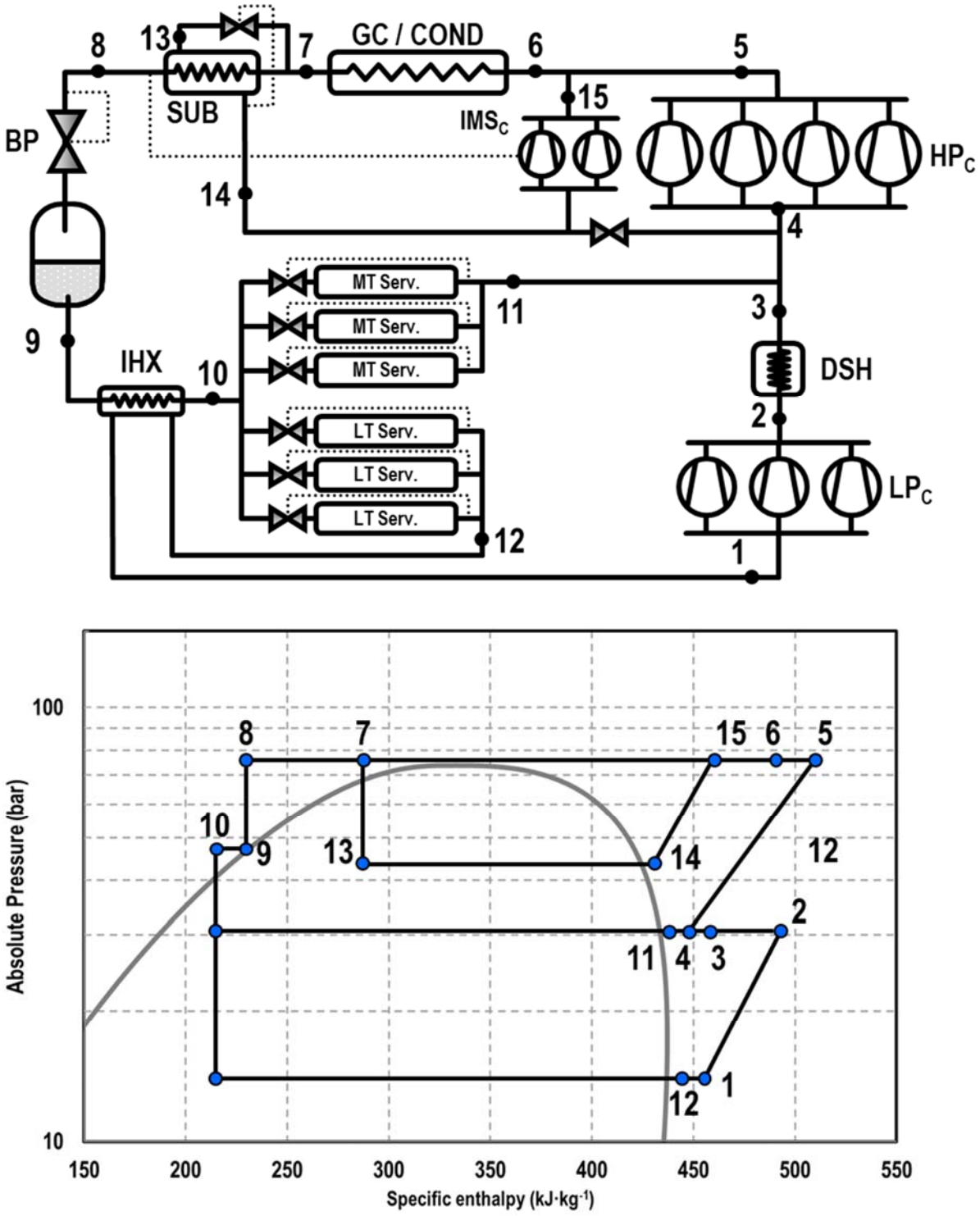

Figure 2. Schematic diagram and Ph diagram of refrigeration booster with integrated mechanical subcooler

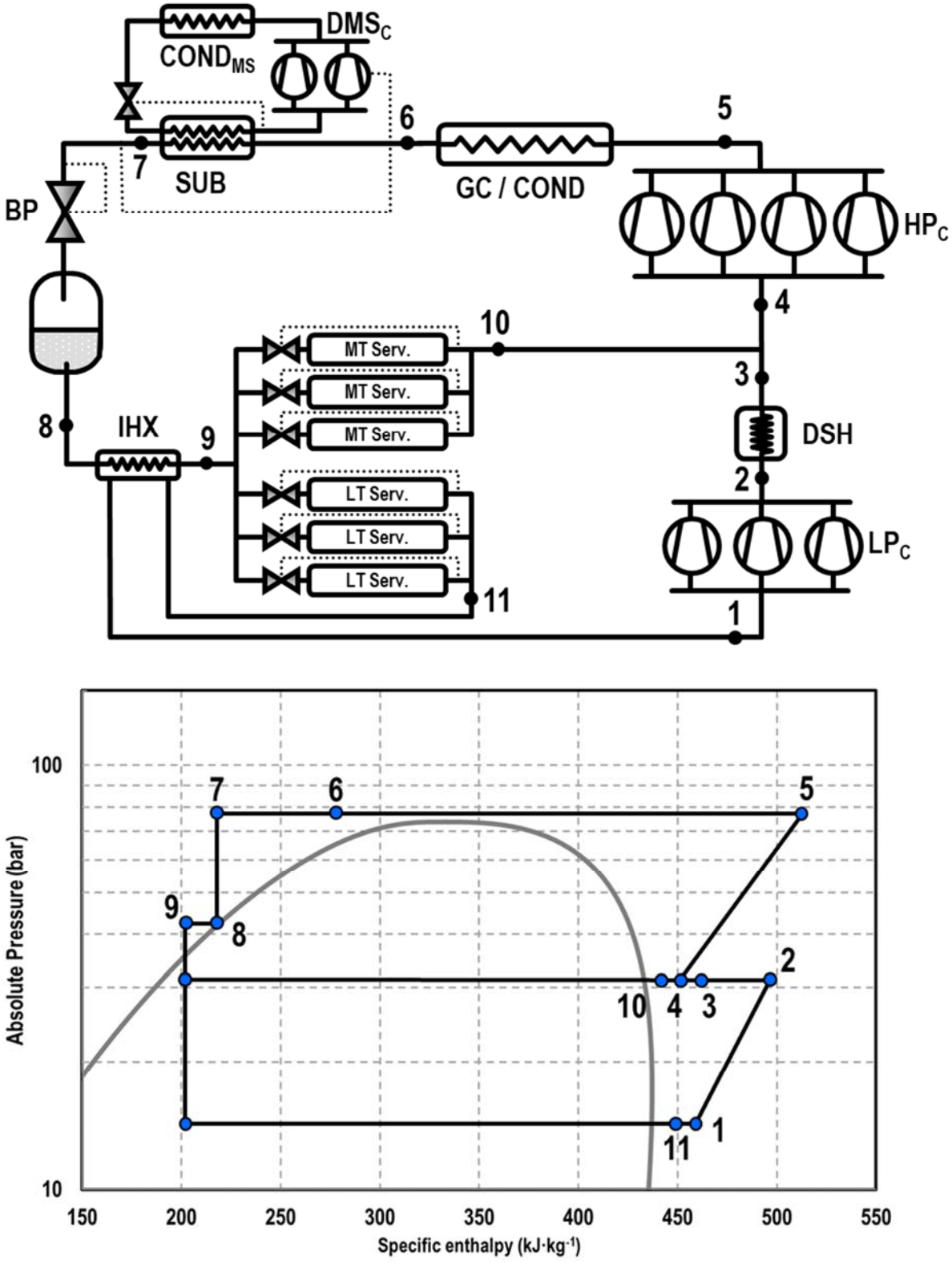

Figure 3. Schematic diagram and Ph diagram of refrigeration booster with dedicated mechanical subcooler

2.2. Compressor's performance data

To evaluate the energy performance of the systems the compressor's performance was obtained from the data provided by compressor manufacturers. CO_2 ones were selected from Bitzer's and R-290 from Dorin's

selection software. This way, Eq. (1) is used to compute volumetric efficiency (η_V) and Eq. (2) and Eq. (3) to calculate the overall efficiency (η_G). The equations used for each compressor rack and the adjustment coefficients are detailed in Table 1, where it is differentiated the operation of the HP_C and PC/IMS_C compressors between subcritical and transcritical modes, as recommended by manufacturers. Deviation of fitted equations from manufacturer's ones is below 0.01%.

$$\eta_V = a_0 + a_1 \cdot p_{suc} + a_2 \cdot p_{dis} + a_3 \cdot \left(\frac{p_{dis}}{p_{suc}}\right) + a_4 \cdot v_{suc} \quad (1)$$

$$\eta_G = b_0 + b_1 \cdot p_{suc} + b_2 \cdot p_{dis} + b_3 \cdot \left(\frac{p_{dis}}{p_{suc}}\right) + b_4 \cdot v_{suc} \quad (2)$$

$$\eta_G = c_0 + c_1 \cdot \left(\frac{p_{dis}}{p_{suc}}\right) + c_2 \cdot \left(\frac{p_{dis}}{p_{suc}}\right)^2 + c_3 \cdot \left(\frac{p_{dis}}{p_{suc}}\right)^3 \quad (3)$$

Compressor's expressions were used to configurate the number of compressors in each rack and in each architecture (results collected in Table 1). The LP_C rack, for all the systems, is composed by three compressors with a displacement of 15.6 $m^3 \cdot h^{-1}$ at nominal speed; HP_C rack by four (17.8 $m^3 \cdot h^{-1}$) compressors; the PC and IMS_C racks by two (9.2 $m^3 \cdot h^{-1}$) and the DMS_C by two (42.81 $m^3 \cdot h^{-1}$) R-290 compressors.

It is also considered that each compressor rack is equipped with an inverter drive to match the heat loads for every external condition. As detailed in Section 3, the minimum frequency for any compressor is set as 30Hz.

2.3. Boundary conditions and assumptions

To evaluate the energy performance of the systems, the following boundary conditions and assumptions were considered:

Characteristics for all architectures:

- Systems were subjected to 140 kW of thermal load at MT with an evaporating level of -6ºC and to 41 kW at LT with an evaporating temperature of -32ºC. These thermal loads were considered constant for all outdoor conditions, since it was considered that the inside of the supermarket was kept at constant temperature and humidity (Emerson, 2010). It is also assumed that the MT cabinets have doors.
- At gas-cooler, 2K was taken as approach temperature with outdoor air in transcritical conditions (Gullo et al., 2018a; Purohit et al., 2018). In subcritical conditions, the temperature difference with air in condenser was of 5K. For the PC system 2K of subcooling degree to guarantee the proper operation of the valve and receiver is considered, and saturation for the others. Also, the desuperheater (DSH) was simulated considering an approach temperature with the environment of 5K.
- Degree of superheat in the MT and LT dry evaporators was of 5K.
- Thermal effectiveness of the IHX at the exit of the vessel was of 65% to guarantee a minimum suction temperature of the LP_C rack.
- All expansion processes were considered isenthalpic.
- Pressure losses in pipes and heat exchangers were neglected.
- All refrigerant properties were computed using Refprop 9.1 database (Lemmon et al., 2013)

For the IMS configuration, in addition to the following considerations, in the SUB a degree of superheat of 5K was considered, being its size determined by the subcooling optimization process. It was modelled by

considering a temperature pinch of 5K between the outlet temperature of subcooler and its evaporating temperature in subcritical conditions and of 2K in transcritical regime. Its thermal effectiveness was considered variable, Eq. (4), being its value inside 57.7 to 90.0% in subcritical conditions and between 87.0 to 92.0% in transcritical conditions. As mentioned, the refrigerant used for subcooling was recompressed by the IMS_C rack, however, when the compression ration of the IMS_C rack was below 1.5 (see section 3), this refrigerant was laminated up to the suction pressure of the HP_C rack. For that condition, the used refrigerant mass flow rate was also obtained by with the subcooling optimization process.

$$\varepsilon_{SUB,IMS} = \frac{t_7 - t_8}{t_7 - t_{13}} \tag{4}$$

In the case of the DMS system, in addition to the general characteristics, the subcooler was modelled considering a constant value of thermal effectiveness of 60%, Eq. (5), and the condensing temperature of the R-290 cycle was obtained with 5K temperature difference with air temperature. Also, the R-290 evaporator was evaluated with a degree of superheat of 5K.

$$\varepsilon_{SUB,DMS} = \frac{t_6 - t_7}{t_6 - t_{O,DMS}} \tag{5}$$

3. Component limitations, optimization and working modes

To be as close as possible to reality and obtain the highest approximation to the real operation of the systems, manufacturer's operating elements limitations were included in the analysis, as previously described by Catalán-Gil et al. (2018), they being;

- Minimum compression ratio for any compressor was of 1.5.
- Minimum pressure difference in any expansion valve was set to 3.5 bar.
- Maximum pressure at the inlet of PC and IMS_C compressors was lower than 55 bar.
- Minimum pressure of the vessel of 35 bar.
- Minimum compressor frequency of 30Hz.

Those restrictions move the real operation of the systems little away from the maximum thermodynamic performance of the cycles, but they are needed to establish a fair comparison scenario.

The evaluation of the systems calculated the best performing operating condition, in terms of maximum COP, restricted to the previously mentioned limitations from outdoor temperatures from 0 to 40ºC. Since the mode of operation of any cycle is bonded to the heat rejection level, the systems were evaluated in subcritical condition, in transitional condition as described by Catalán-Gil et al. (2018) and Danfoss (2012) and in transcritical condition. The best performing situation was selected for each outdoor temperature. To select the optimum working condition different parameters were optimized in each cycle configuration, bonded to fulfil the heat loads to the MT and LT services.

- PC system (Figure 1): heat rejection pressure in transcritical and transitional conditions (point 7, Figure 1) and vessel pressure (point 9/13, Figure 1). At low outdoor temperatures, where the PC rack cannot operate, only vessel pressure, since high pressure was fixed by condensation.
- IMS system (Figure 2): heat rejection pressure in transcritical and transitional conditions, optimum subcooling degree ($t_7 - t_8$, Figure 2) and optimum evaporation temperature in the subcooler or suction pressure of IMS_C rack. At low outdoor temperatures, where the IMS_C cannot operate the optimum subcooling degree was also evaluated, and the high pressure was established by condensation.

- DMS system (Figure 3): heat rejection pressure in transcritical and transitional conditions (point 7, Figure 3) and optimum subcooling degree ($t_6 - t_7$, Figure 3). In subcritical conditions only the optimum subcooling degree was optimized.

Component limitations and modes of operation established the best performing conditions for each cycle at each outdoor temperature, as detailed in Tables 2 to 4. The PC cycle operates in subcritical up to 22.65ºC of outdoor temperature, in transition up to 28.50ºC and then in transcritical. The FG valve operates from 0.00 to 8.58ºC and the parallel compressor from 8.58ºC on. Pressures were fixed or floating depending on the restrictions, as detailed in Table 2

. The IMS architecture works in subcritical up to 23.75ºC, in transition up to 28.60ºC and then in transcritical. The IMS_C rack only operates from 6.63ºC on. Again, pressures were fixed or floating according to limitations, as collected in Table 3. Finally, the DMS cycle operates in subcritical up to 23.5ºC, in transition up to 28.60ºC and then in transcritical. The DMS_C rack operates from 8.12ºC on. Also, pressures were fixed or floating according to restrictions, as presented in Table 4.

4. Energy performance results

4.1. Optimum parameters

Figure 4 summarises the optimum working conditions representing the outlet state at the gas-cooler/condenser (dashed line) and outlet state of the subcooler (continuous line) for all outdoor temperatures. The evaluated limits are detailed with a circle, for the operation at t_{env}=40ºC, and with a square, for t_{env}=0ºC. The optimum conditions of CO_2 at the exit of gas-cooler for the PC system (black line) follow the trend of industrial controllers (Danfoss, 2011), however architectures with subcooling present a large enthalpy reduction through the subcooler. Accordingly, the standard controllers must be redesigned for these cycles.

Figure 5 depicts the optimum subcooling degrees for each configuration. It is observed that IMS cycle always operate with subcooling, it varying between 8.9K at t_{env}=0ºC to 22.7K at t_{env}=40ºC. However, the DMS system only operates with the subcooling system for environment temperatures higher than 8.15ºC, it varying between 9.30 to 30.85K.

In terms of powers, to illustrate the operation of the systems and size of components, Table 5 collects main pressures, compressor's power consumption, heat transfer in principal heat exchangers and COP of systems for t_{env}=0, 20 and 40ºC. As it can be observed, the degree of subcooling fix a maximum heat transfer rate of 97.5 kW in the DMS and of 76.3 kW in the IMS systems (at t_{env}=40ºC). Another important aspect is the total heat rejection to the environment, which is nearly constant for all the systems. Furthermore, as it can be seen each architecture obtains the best COP for different outdoor temperatures. At low values the PC results the most beneficial, at 20ºC the IMS and at warmest conditions the DMS one.

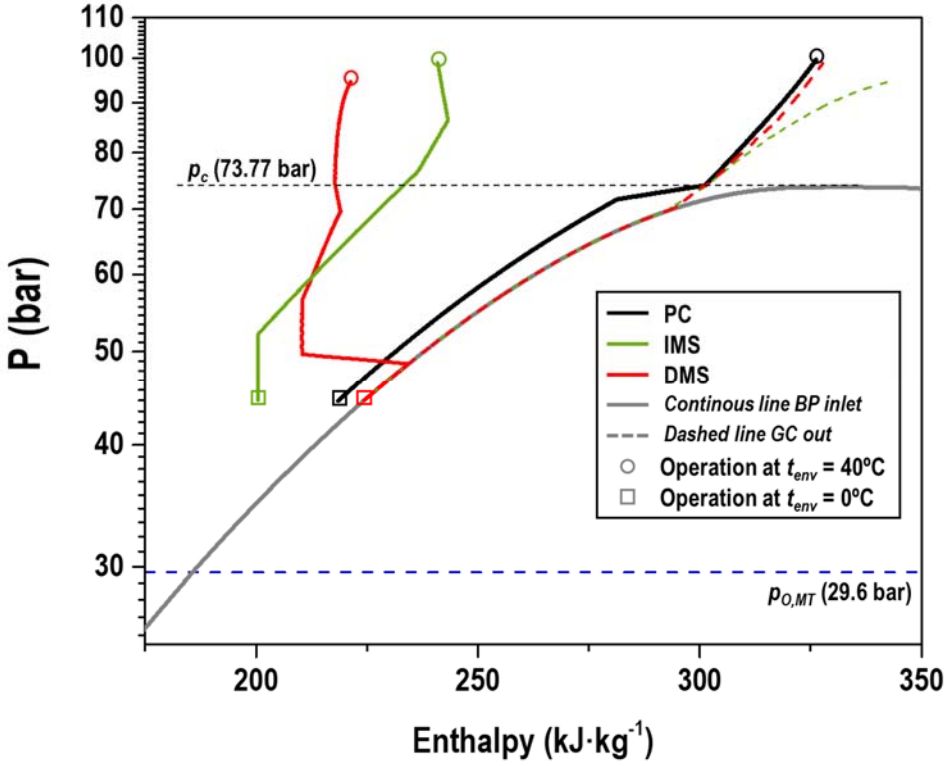

Figure 4. Enthalpy at gas-cooler/condenser outlet (dashed line) and at back-pressure inlet (continuous line) at optimum conditions

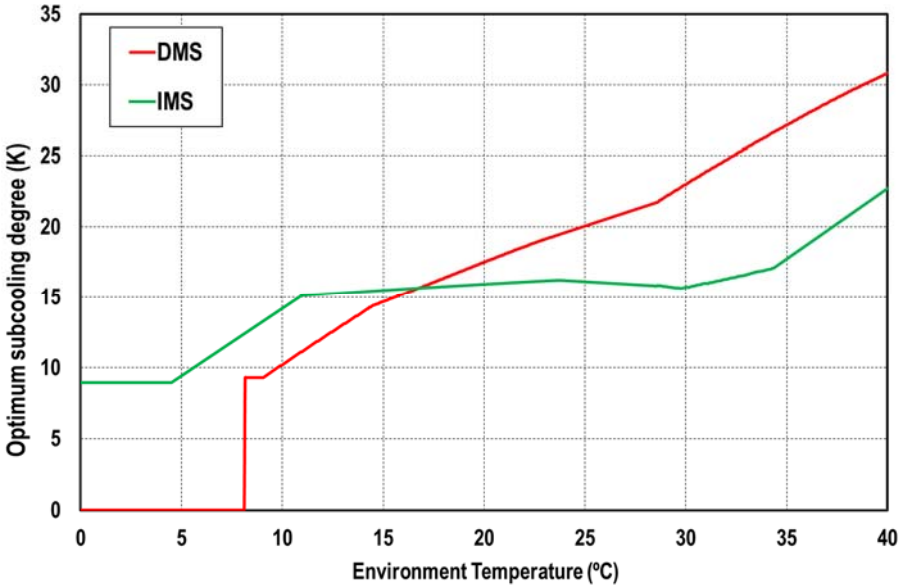

Figure 5. Optimum subcooling degrees in subcooler for DMS and IMS

4.2. Best performing conditions

Figure 6 presents the COP evolutions for the systems (PC Eq. (6), IMS Eq. (7), DMS Eq. (8)) and Figure 7 the percentage difference of DMS and IMS in relation to PC configuration. The COP values for each configuration are detailed in Table 2 to 4 according to the polynomial relation expressed by Eq. (9). PC system offers higher COP values at low temperatures (up to 2.7ºC in relation to IMS and up to 3.75ºC respect the DMS). The temperature region from 2.7ºC to 22.15ºC is dominated by the IMS system, reaching COP increments up to 8.4% in relation to the PC system. Finally, for temperatures higher than 22.15ºC the

DMS architecture gets the highest efficiency, with a maximum increment of 16.5% in relation to the PC system. As observed in Figure 7 and Table 5, each system obtains the highest COP values for each section of outdoor temperatures: PC system is appropriate for cold environments, IMS for tempered and warm zones and DMS for hot conditions.

$$COP_{PC} = \frac{\dot{Q}_{O,MT} + \dot{Q}_{O,LT}}{P_{C,LP_C} + P_{C,HP_C} + P_{C,PC}} \quad (6)$$

$$COP_{IMS} = \frac{\dot{Q}_{O,MT} + \dot{Q}_{O,LT}}{P_{C,LP_C} + P_{C,HP_C} + P_{C,IMSC}} \quad (7)$$

$$COP_{DMS} = \frac{\dot{Q}_{O,MT} + \dot{Q}_{O,LT}}{P_{C,LP_C} + P_{C,HP_C} + P_{C,DMSC}} \quad (8)$$

$$COP = d_0 + d_1 \cdot t_{env} + d_2 \cdot {t_{env}}^2 + d_3 \cdot {t_{env}}^3 \quad (9)$$

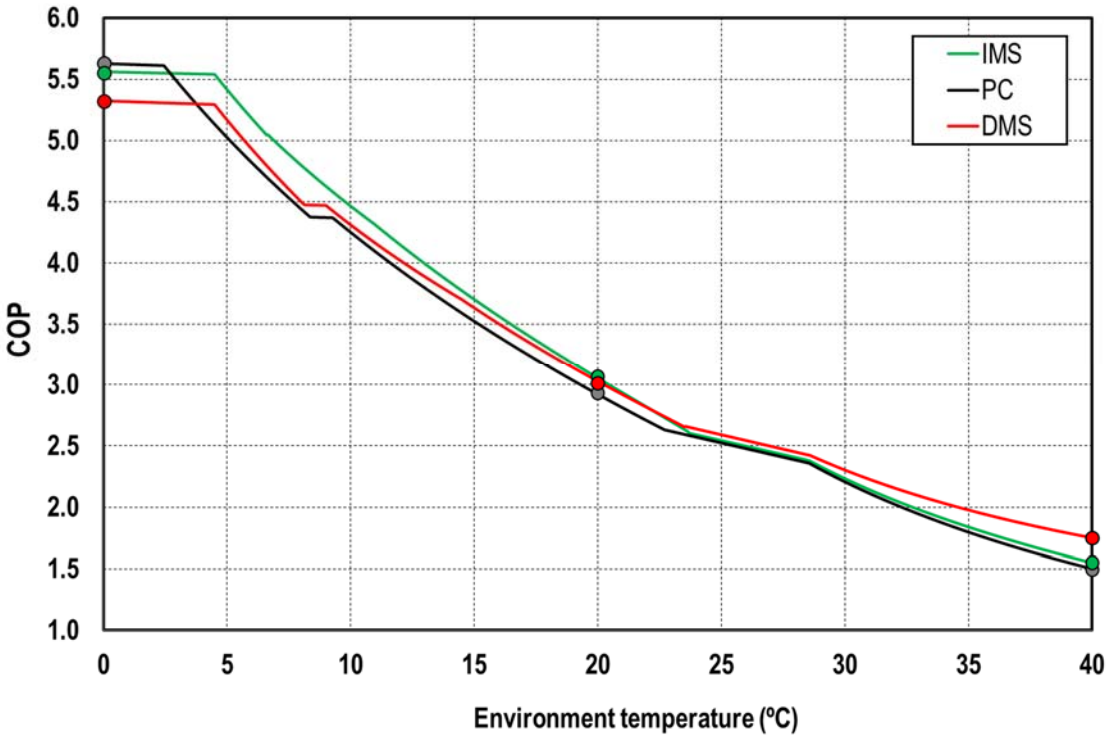

Figure 6. COP vs. environment temperature for PC, DMS and IMS systems

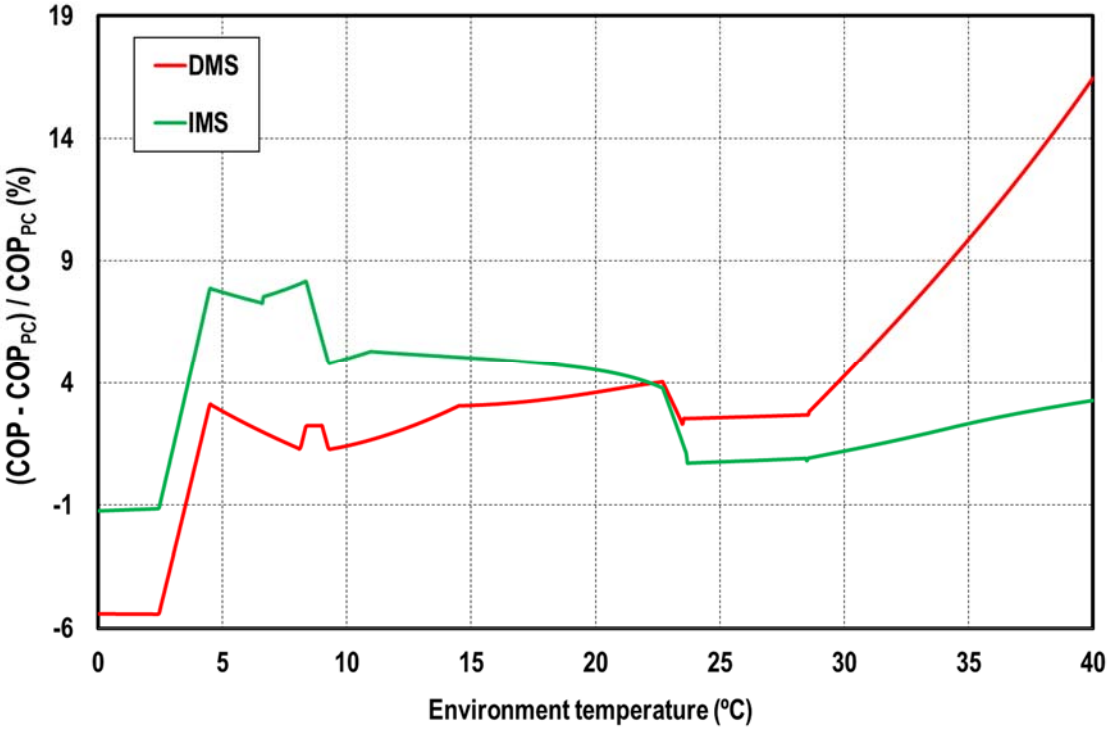

Figure 7. COP percentage difference of DMS and IMS systems in relation to PC

5. Energy improvements

COP values (Tables 2 to 4) are used to calculate the annual energy consumption of the systems in a real application according to Eq. (10). This calculation gets as inputs the hourly outdoor temperature of a city from the typical meteorological year defined by EnergyPlus (2018) and the design thermal loads to the MT (140kW) and LT (41kW) services. To simplify the calculation the load factor (LF) is considered as 100% from 7:00 a.m. to 10:00 p.m., corresponding to the opening hours of a typical supermarket, and as 50% from 10:00 p.m. to 7:00 a.m., representing the closing schedule of the commerce, where the cabinets are not opened due to the absence of customers (Catalán-Gil et al., 2018). This calculation considers that the indoor conditions of the supermarket are constant thorough the entire year. Differences in energy consumption in relation to PC system (Eq. 11 and 12) were contrasted with the load factor benchmark proposed by Minetto et al. (2016), being the maximum difference between both load factor criterions below 0.41%.

$$E\ (kWh) = \sum_{m=1}^{12} \sum_{h=1}^{24} \frac{\dot{Q}_{O,MT} + \dot{Q}_{O,LT}}{COP_i(t_{env})} \cdot \frac{LF}{100} \cdot D_m \quad (10)$$

Using Eq. (10) the annual energy consumption difference of DMS and IMS systems in relation to PC configuration has been calculated using Eq. (11) and (12).

$$\Delta E_{IMS}\ (\%) = \frac{E_{PC} - E_{IMS}}{E_{IMS}} \cdot 100 \quad (11)$$

$$\Delta E_{DMS}\ (\%) = \frac{E_{PC} - E_{DMS}}{E_{DMS}} \cdot 100 \quad (12)$$

Calculations of annual energy consumption have been made by 282 locations in Europe and 395 cities of Asia, some of the representative cities collected in Table 6, which have been classified according to their annual average temperature as cold ($\bar{t}_{env} \in 0 - 10$ºC), tempered ($\bar{t}_{env} \in 10 - 18$ºC), warm ($\bar{t}_{env} \in 18 - 23$ºC) and hot ($\bar{t}_{env} \in 23 - 28$ºC) regions. As logical, the annual energy consumption increases with increased average temperature, and it can be seen that this value is nearly double between cold places (Stockholm, $\bar{t}_{env}$=6.5ºC) and hot locations (Bangkok, $\bar{t}_{env}$=28.5ºC). In terms of percentage COP in relation to the reference system, DMS system offers energy benefits for locations with environment temperature higher than 14.27ºC (Prague), with energy reductions nearly linear with the annual average temperature, but the increments are only representative for places with annual temperature from 17.9ºC (Athens). Although the number of hours in operation of the DMS compressors are similar to PC compressors, that indicates that from an economic point of view, the DMS system is only interesting for warm and hot regions. However, the IMS system brings about energy reduction for all climate conditions. In fact, for the coldest place (Stockholm), the IMS configuration allows energy reductions of 3.1%, reaches the maximum benefits in tempered climates (London, -5.3%) and its benefit is reduced at warm and hot locations. Again, the number of hours of operation of the IMS_C rack is similar to the PC one, indicating that this system is very interesting for mild climate conditions.

To extend the analysis to all the locations considered in this work, the energy results are represented using contour maps. Figure 8 represents the energy improvement of DMS (left) and IMS (right) systems for Europe and Figure 9 for Asia. With red dots are represented the cities considered in the calculation and in green dots the locations that are detailed in Table 6.e.

In relation to the DMS architecture, it can be seen that it does not offer energy benefit for cold regions, such as Northern Europe, Northern Asia and inside part to the west of China. However, its improvements rise when going away from those regions. In Europe, the benefits rise for locations near the Mediterranean Sea and even the British Islands. In countries such as Spain, Italy, France and Greece the annual energy

improvement is between 1.5 to 3.5%. In Asia, the benefits are also extended to locations near the see, but the highest improvements are located in India, with annual improvements from 3 to 6%.

The IMS configuration, presents a different trend, although this system is positive for all considered locations, the highest improvements are located in regions with cold and tempered climate, In Central Europe and specially the West of British Islands it offers annual improvements between 4 to 6%, and in Asia the inside part of China is the region where the improvements are highest, with annual energy reductions from 4 to 6% too.

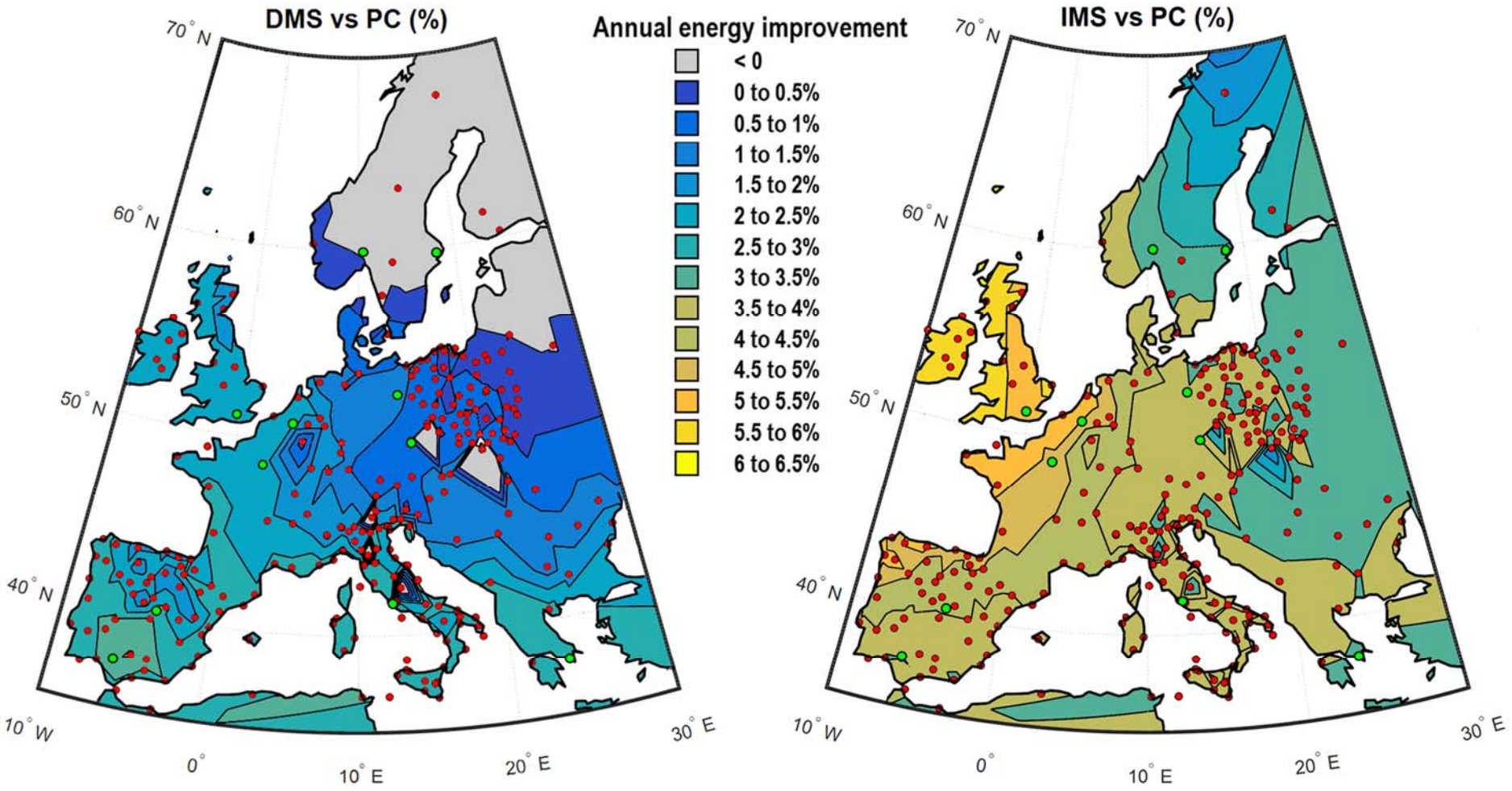

Figure 8. Annual energy benefit of DMS and IMS in relation to PC in Europe (%)

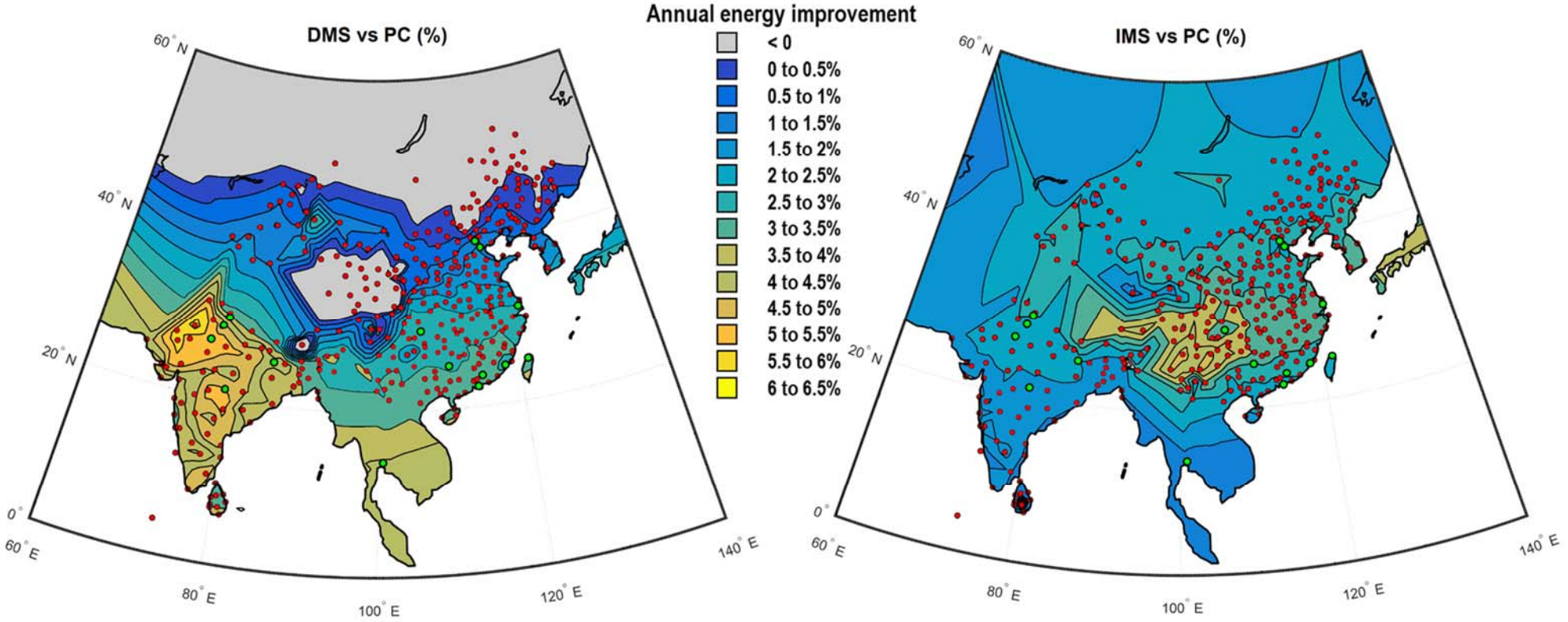

Figure 9. Annual energy benefit of DMS and IMS in relation to PC in Asia (%)

6. Conclusions

This work analyses close to reality the CO_2 booster system with integrated mechanical subcooling and the CO_2 booster with R-290 dedicated mechanical subcooling cycles in relation to the state-of-the-art CO_2 booster system with parallel compression for supermarket applications. The evaluation has considered a typical supermarket application with 140kW and 41kW of thermal loads at medium and low temperature services, respectively. The analysis was based on compressor's performance data provided by manufacturer and real limitations of the elements of the plant (compressor, expansion valves).

The best performing conditions of the cycles have been stablished by optimization of their operating mode (subcritical, transition and transcritical) and their possibilities of operation (use of auxiliary compressors, flash-gas by pass valve,…) over an outdoor temperature range from 0 to 40ºC. It has been concluded that the DMS system only subcools for temperatures higher than 8.15ºC but the IMS uses subcooling for all evaluated range. Both systems only offer COP benefits for outdoor temperatures of 2.7ºC (DMS) and 3.75ºC (IMS), the IMS performs the best at temperatures from 2.7 to 22.15ºC, and the DMS from 22.15ºC on, in relation to the PC configuration.

The systems were subjected to annual energy consumption calculation for 282 locations in Europe and 395 cities of Asia, where the following conclusions were extracted:

- The DMS system does not offer energy benefit for cold climates (Northern Europe, Northern Asia and inside part to the west of China), the best energy improvements are at warm and hot climates, but it offers energy consumption reductions between 1.5 to 3.5% annually in Southern Europe (Spain, Italy, France and Greece) and in British Islands. The best improvements are located in India with annual energy reductions between 3 to 6%.
- The IMS configuration is positive for all locations, the highest improvements located in regions with tempered climate. In Central Europe and West of British Islands it offers annual reductions between 4 to 6% and in central China from 4 to 6%.

Accordingly, the general conclusion is that the booster systems with subcooling are feasible to be implemented in supermarket refrigeration systems, the IMS is a suitable system for tempered climates and the DMS is restricted to regions with warm and hot climate conditions.

Acknowledgements

Authors gratefully acknowledge Ministerio de Economía y Competitividad of Spain (project ENE2014-53760-R.7, grant FPI BES-2015-073612), Ministerio de Educación, Cultura y Deporte (grant FPU16/00151) and Jaume I University of Spain (project UJI-B2017-06) for financing this research work

References

Catalán-Gil, J., Sánchez, D., Llopis, R., Nebot-Andrés, L., Cabello, R., 2018. Energy Evaluation of Multiple Stage Commercial Refrigeration Architectures Adapted to F-Gas Regulation. Energies 11, 1915.

Cecchinato, L., Chiarello, M., Corradi, M., Fornasieri, E., Minetto, S., Stringari, P., Zilio, C., 2009. Thermodynamic analysis of different two-stage transcritical carbon dioxide cycles. International Journal of Refrigeration 32, 1058-1067.

Dai, B., Liu, S., Li, H., Sun, Z., Song, M., Yang, Q., Ma, Y., 2018. Energetic performance of transcritical CO 2 refrigeration cycles with mechanical subcooling using zeotropic mixture as refrigerant. Energy 150, 205-221.

Dai, B., Liu, S., Zhu, K., Sun, Z., Ma, Y., 2017. Thermodynamic performance evaluation of transcritical carbon dioxide refrigeration cycle integrated with thermoelectric subcooler and expander. Energy 122, 787-800.

Danfoss, 2011. Controller to regulate CO2 gas pressure. Available online: http://files.danfoss.com/TechnicalInfo/Dila/01/RS8FM502.pdf (accessed on 17 December 2018).

Danfoss, 2012. Electronically Operated Expansion Valve for CO2 Type AKVH. 2012. Available online: http://files.danfoss.com/technicalinfo/dila/01/DKRCCPDVA1D302SmartconnectorAKVH.pdf (last acces October 5th).

Emerson, 2010. Refrigerant Choices for Commercial Refrigeration Finding the Right Balance. www.emersonclimate.com/europe/documents/resources/tge124_refrigerant_report_en_1009.pdf.

EnergyPlus, 2018. Weather data. .

European Commission, 2014. Regulation (EU) No 517/2014 of the European Parliament and of the Council of 16 April 2014 on fluorinated greenhouse gases and repealing Regulation (EC) No 842/2006.

Girotto, S., 2017. Improved transcritical CO2 refrigeration systems for warm climates. , Proceedings of the 7th IIR Ammonia and CO2 Refrigeration Technologies Conference, 11th - 13th May. Ohrid, Macedonia .

Gullo, P., Cortella, G., 2016. Comparative Exergoeconomic Analysis of Various Transcritical R744 Commercial Refrigeration Systems, in: Ljubljana, U.o. (Ed.), ECOS 2016 - The 29th International conference on efficiency, cost, optimization, simulation and environmental impact of energy systems., Portoroz, Slovenia.

Gullo, P., Hafner, A., Banasiak, K., 2018a. Transcritical R744 refrigeration systems for supermarket applications: Current status and future perspectives. International Journal of Refrigeration 93, 269-310.

Gullo, P., Hafner A., 2017. Thermodynamic performance assessment of a CO2 supermarket refrigeration system with auxiliary compression economization by using advanced exergy analysis. International Journal of Thermodynamics 20, 220-227.

Gullo, P., Tsamos, K.M., Hafner, A., Banasiak, K., Ge, Y.T., Tassou, S.A., 2018b. Crossing CO2 equator with the aid of multi-ejector concept: A comprehensive energy and environmental comparative study. Energy 164, 236-263.

Karampour, M., Sawalha, S., 2017. Energy efficiency evaluation of integrated CO2 trans-critical system in supermarkets: A field measurements and modelling analysis. International Journal of Refrigeration 82, 470-486.

Karampour, M., Sawalha, S., 2018. State-of-the-art integrated CO 2 refrigeration system for supermarkets: A comparative analysis. International Journal of Refrigeration 86, 239-257.

Lemmon, E.W., Huber, M.L., McLinden, M.O., 2013. REFPROP, NIST Standard Reference Database 23, v.9.1. National Institute of Standards, Gaithersburg, MD, U.S.A.

Llopis, R., Nebot-Andrés, L., Sánchez, D., Catalán-Gil, J., Cabello, R., 2018. Subcooling methods for CO2 refrigeration cycles: A review. International Journal of Refrigeration 93, 85-107.

Llopis, R., Sanz-Kock, C., Cabello, R., Sánchez, D., Torrella, E., 2015. Experimental evaluation of an internal heat exchanger in a CO2 subcritical refrigeration cycle with gas-cooler. Applied Thermal Engineering 80, 31-41.

Minetto, S., Rossetti, A., Girotto, S., Marinetti, S., 2016. Seasonal performance of supermarket refrigeration systems, in: IIR (Ed.), 12th IIR Gustav Lorentzen Conference on Natural Refrigerants (GL2016). IIR, Édimbourg, United Kingdom.

Nebot-Andrés, L., Llopis, R., Sánchez, D., Catalán-Gil, J., Cabello, R., 2017. CO2 with Mechanical Subcooling vs. CO2 Cascade Cycles for Medium Temperature Commercial Refrigeration Applications Thermodynamic Analysis. Applied Sciences 7, 955.

Purohit, N., Gullo, P., Dasgupta, M.S., 2017. Comparative Assessment of Low-GWP Based Refrigerating Plants Operating in Hot Climates. Energy Procedia 109, 138-145.

Purohit, N., Sharma, V., Sawalha, S., Fricke, B., Llopis, R., Dasgupta, M.S., 2018. Integrated supermarket refrigeration for very high ambient temperature. Energy 165, 572-590.

Sawalha, S., 2013. Investigation of heat recovery in CO2 trans-critical solution for supermarket refrigeration. International Journal of Refrigeration 36, 145-156.

Sawalha, S., Piscopiello, S., Karampour, M., Manickam, L., Rogstam, J., 2017. Field measurements of supermarket refrigeration systems. Part II: Analysis of HFC refrigeration systems and comparison to CO2 trans-critical. Applied Thermal Engineering 111, 170-182.

TABLES

Table 1. Performance data of compressors. Obtained from manufacturer data.

	Model	$\dot{V}_G$ at 1450 rpm ($m^3 \cdot h^{-1}$)	Number of compressors	Subcritical operation				Transcritical operation			
LP_C	Bitzer 4ESL-9K	15.6	3	η_V	Ec. [1]	η_G	Ec. [2]				
	Refrigerant: R-744			a_0	1.14985663	b_0	0.61678183				
				a_1	0.00285336	b_1	-0.00824113				
				a_2	-0.00451612	b_2	0.01143067				
				a_3	-0.04218443	b_3	-0.14816646				
				a_4	-3.24182999	b_4	5.35184767				
HP_C	Bitzer 4CTC-30K	17.8	4	η_V	Ec. [1]	η_G	Ec. [3]	η_V	Ec. [1]	η_G	Ec. [2]
	Refrigerant: R-744			a_0	0.96562667	c_0	-0.30239969	a_0	1.0922959	b_0	0.84748849
				a_1	0.00478809	c_1	1.18485292	a_1	0.00105465	b_1	-0.00647244
				a_2	-0.00264638	c_2	-0.46751257	a_2	-0.00227064	b_2	0.00190887
				a_3	-0.03228407	c_3	0.06039427	a_3	-0.02000997	b_3	-0.08083942
				a_4	-0.68096605	c_4	-	a_4	-4.2528302	b_4	5.32100343
PC / IMS_C	Bitzer 4JTC-10K-40P	9.2	2	η_V	Ec. [1]	η_G	Ec. [2]	η_V	Ec. [1]	η_G	Ec. [2]
	Refrigerant: R-744			a_0	0.79042139	b_0	1.04277933	a_0	0.85390033	b_0	0.74453886
				a_1	0.00841379	b_1	-0.00871981	a_1	0.0083094	b_1	0.00045915
				a_2	-0.00228299	b_2	0.00352851	a_2	-0.0033132	b_2	0.00028444
				a_3	-0.05525721	b_3	-0.06160335	a_3	0.00848023	b_3	-0.033457
				a_4	5.02592536	b_4	-14.7718425	a_4	-5.39769047	b_4	-1.69059837
DMS	Dorin HEX1201CC	42.81	2	η_V	Ec. [1]	η_G	Ec. [2]				
	Refrigerant: R-290			a_0	0.36760973	b_0	1.012177528				
				a_1	-0.06784174	b_1	0.013245153				
				a_2	0.06782300	b_2	-0.002583983				
				a_3	-0.17946704	b_3	-0.003944654				
				a_4	2.41571076	b_4	-1.170750682				

Table 2. Performance data of parallel compression with flash gas by-pass valve system

Section	t_{env} min (ºC)	t_{env} max (ºC)	FG	PC	Operation and limitations	d_0	d_1	d_2	d_3
1	0	2.5	ON	OFF	- subcritical - PC off (CR_{PC}<1.5) - p_{ves} = 35 bar - p_{cond} = 44.5 bar ($CR_{C,MT}$=1.5)	5.629	$-7.013 \cdot 10^{-3}$	$5.036 \cdot 10^{-5}$	$-9.046 \cdot 10^{-7}$
2	2.5	8.58	ON	OFF	- subcritical - PC off (CR_{PC}<1.5) - p_{ves} = 35 bar - p_{cond} = floating	6.273	$-2.944 \cdot 10^{-1}$	$1.024 \cdot 10^{-2}$	$-2.595 \cdot 10^{-4}$
3	8.58	9.27	OFF	ON	- subcritical - p_{ves} = 35 bar - p_{cond} = 52.45 bar (CR_{PC}=1.5)	4.761	$-1.212 \cdot 10^{-1}$	$1.312 \cdot 10^{-2}$	$-4.946 \cdot 10^{-4}$
4	9.27	22.65	OFF	ON	- subcritical - p_{ves} = floating (optimized) - p_{cond} = floating	6.258	$-2.472 \cdot 10^{-1}$	$5.280 \cdot 10^{-3}$	$-6.283 \cdot 10^{-5}$
5	22.65	28.5	OFF	ON	- transition - p_{ves} = floating (optimized) - p_{gc} = floating (optimized)	3.689	$-4.653 \cdot 10^{-2}$	$-4.493 \cdot 10^{-15}$	$5.937 \cdot 10^{-17}$
6	28.5	40	OFF	ON	- transcritical - p_{ves} = floating (optimized) - p_{gc} = floating (optimized)	11.26	$-5.955 \cdot 10^{-1}$	$1.280 \cdot 10^{-2}$	$-1.004 \cdot 10^{-4}$

Table 3. Performance data of booster with integrated mechanical subcooling system

Section	t_{env} min (ºC)	t_{env} max (ºC)	IMS_C	Operation and limitations	d_0	d_1	d_2	d_3
1	0	4.49	OFF	- subcritical - AUX COMP off (CR_{AUX}<1.5) - p_{ves} = 35 bar - p_{cond} = 44.5 bar ($CR_{C,MT}$=1.5)	5.560	$-4.840 \cdot 10^{-3}$	$3.217 \cdot 10^{-5}$	$-5.452 \cdot 10^{-7}$
2	4.49	6.63	OFF	- subcritical - AUX COMP off (CR_{AUX}<1.5) - p_{ves} = 35 bar - p_{cond} = floating	6.873	$-3.502 \cdot 10^{-1}$	$1.341 \cdot 10^{-2}$	$-3.539 \cdot 10^{-4}$
3	6.63	23.75	ON	- subcritical - p_{ves} = floating (optimized) - p_{cond} = floating	6.397	$-2.272 \cdot 10^{-1}$	$3.769 \cdot 10^{-3}$	$-3.828 \cdot 10^{-5}$
4	23.75	28.6	ON	- transition - p_{ves} = floating (optimized) - p_{gc} = floating (optimized)	3.696	$-4.591 \cdot 10^{-2}$	$9.558 \cdot 10^{-15}$	$-1.235 \cdot 10^{-16}$
5	28.6	40	ON	- transcritical - p_{ves} = floating (optimized) - p_{gc} = floating (optimized)	11.54	$-6.263 \cdot 10^{-1}$	$1.391 \cdot 10^{-2}$	$-1.124 \cdot 10^{-4}$

Table 4. Performance data of booster with dedicated mechanical subcooling system

Section	t_{env} min (ºC)	t_{env} max (ºC)	DMS_C	Operation and limitations	d_0	d_1	d_2	d_3
1	0	4.49	OFF	- subcritical - AUX COMP off (CR_{AUX}<1.5) - p_{ves} = 44.5 bar (BP fully open) - p_{cond} = 44.5 bar ($CR_{C,MT}$=1.5)	5.325	$-6.923 \cdot 10^{-3}$	$4.987 \cdot 10^{-5}$	$-8.211 \cdot 10^{-7}$
2	4.49	8.12	OFF	- subcritical - AUX COMP off (CR_{AUX}<1.5) - p_{ves} = floating (BP fully open) - p_{cond} = floating bar	6.655	$-3.582 \cdot 10^{-1}$	$1.383 \cdot 10^{-2}$	$-3.410 \cdot 10^{-4}$
3	8.12	9.3	ON	- subcritical - p_{ves} = floating (optimized) - p_{cond} = 49.65 bar - DMS_C frequency 30Hz - $p_{cond,AUX}$ = 4.7 bar ($\Delta p_{EXV,DMS}$=3.5 *bar*)	4.520	$-5.742 \cdot 10^{-3}$	$3.726 \cdot 10^{-5}$	$-4.087 \cdot 10^{-7}$
4	9.3	14.33	ON	- subcritical - p_{ves} = floating (optimized) - p_{cond} = floating - $p_{cond,AUX}$ = 4.7 bar ($\Delta p_{EXV,DMS}$=3.5 *bar*)	6.488	$-2.971 \cdot 10^{-1}$	$9.523 \cdot 10^{-3}$	$-1.576 \cdot 10^{-4}$
5	14.33	23.5	ON	- subcritical - p_{ves} = floating (optimized) - p_{cond} = floating - $p_{cond,AUX}$ = floating	6.640	$-2.878 \cdot 10^{-1}$	$7.240 \cdot 10^{-3}$	$-9.379 \cdot 10^{-5}$
6	23.5	28.6	ON	- transition - p_{ves} = floating (optimized) - p_{gc} = floating (optimized) - $p_{cond,AUX}$ = floating	3.766	$-4.698 \cdot 10^{-2}$	$3.950 \cdot 10^{-15}$	$-5.111 \cdot 10^{-17}$
7	28.6	40	ON	- transcritical - p_{ves} = floating (optimized) - p_{gc} = floating (optimized) - $p_{cond,AUX}$ = floating	9.711	$-4.863 \cdot 10^{-1}$	$1.037 \cdot 10^{-2}$	$-7.979 \cdot 10^{-5}$

Table 5. Main operating parameters of the systems at t_{env} = 0, 20 and 40ºC attending a cooling demand of 140kW at MT and 41kW at LT

		PRESSURES			COMPRESSOR'S POWER CONSUMPTION				HX HEAT TRANSFER							
t_{env} (ºC)	system	p_{GC} (bar)	$p_{suc,IMS/PC}$ (bar)	p_{ves} (bar)	$P\ LP_C$ (kW)	$P\ HP_C$ (kW)	$P\ PC/IMS_C$ (kW)	$P\ DMS_C$ (kW)	$Q_{IHX,LT}$ (kW)	Q_{DSH} (kW)	$Q_{GC/K}$ (kW)	SUB (K)	Q_{SUB} (kW)	$Q_{K,MS}$ (kW)	$Q_{GC/K} + Q_{K,MS}$ (kW)	COP
0	PC	44.4	0.0	35.0	9.6	22.6	0.0	-	2.5	11.6	198.8	-	-	-	198.8	5.63
	DMS	44.5	0.0	44.5	10.8	23.2	-	0.0	3.8	14.2	198.6	0	0.0	0.0	198.6	5.32
	IMS	44.5	0.0	35.0	9.6	23.0	0.0	-	0.6	11.6	198.4	8.9	17.7	-	198.4	5.56
20	PC	67.4	41.9	41.9	10.5	44.5	6.9	-	3.5	9.0	228.6	-	-	-	228.6	2.92
	DMS	64.3	0.0	40.9	10.3	41.5	-	8.0	3.3	8.8	175.5	17.5	46.5	54.5	230.0	3.03
	IMS	64.3	42.9	42.5	10.6	42.2	6.5	-	0.8	9.1	225.9	15.9	44.1	-	225.9	3.06
40	PC	99.6	53.8	53.8	12.2	84.3	23.9	-	5.2	7.3	280.9	-	-	-	280.9	1.50
	DMS	94.6	0.0	43.2	10.6	71.0	-	21.7	3.6	5.2	157.9	30.9	97.5	119.3	277.2	1.75
	IMS	98.9	55.0	51.3	11.8	81.3	23.5	-	1.1	6.7	279.1	22.7	76.3	-	279.1	1.55

Table 6. Average temperature and annual energy consumption for selected cities

City	Country	Long (º)	Lat (ºC)	Annual Temp (ºC)	E_{PC} (MW·h)	E_{DMS} (MW·h)	E_{IMS} (MW·h)	$(E_{PC}- E_{DMS})/E_{PC}\cdot 100$ (%)	$(E_{PC}- E_{IMS})/E_{PC}\cdot 100$ (%)	PC annual hours (%)	IMS annual hours (%)	DMS annual hours (%)
Region type: Cold, annual average temperature from 0 to 10ºC*												
Stockholm	SWE	59.65	17.95	6.5	306.6	307.4	297.3	-0.3	3.1	42	48	43
Oslo	NOR	59.90	10.62	6.7	308.8	309.0	298.9	-0.1	3.2	40	49	43
Prague	CZE	50.08	14.27	8.1	321.6	319.9	310.4	0.5	3.5	49	52	50
Berlin	DEU	52.47	13.38	9.8	335.7	331.6	322.4	1.2	4.0	53	58	54
Region type: Tempered, annual average temperature from 10ºC to 18ºC*												
London	GBR	51.15	-0.17	10.2	335.4	327.8	317.6	2.3	5.3	56	66	59
Brussels	BEL	50.90	4.52	10.3	336.3	329.3	319.5	2.1	5.0	57	65	59
Paris	FRA	48.72	2.40	11.1	349.4	341.3	332.3	2.3	4.9	57	64	59
Beijing	CHN	39.78	116.47	12.6	389.5	383.8	379.7	1.5	2.5	62	67	64
Tianjin	CHN	39.07	117.07	12.9	390.2	384.8	380.8	1.4	2.4	63	65	64
Madrid	ESP	40.40	-3.67	14.3	393.3	382.6	376.7	2.7	4.2	72	84	74
Rome	ITA	41.78	12.22	15.8	410.9	400.0	394.8	2.7	3.9	84	96	86
Shanghai	CHN	31.38	121.43	16.7	422.7	411.7	408.4	2.6	3.4	76	84	77
Athens	GRC	37.90	23.72	17.9	438.0	425.5	423.5	2.9	3.3	97	100	98
Region type: Warm, annual average temperature from 18ºC to 23ºC*												
Sevilla	ESP	37.42	-5.90	18.3	451.8	436.2	436.1	3.4	3.5	93	99	94
Chongqing	CHN	29.57	106.47	18.5	445.0	432.3	430.8	2.9	3.2	92	99	95
Guilin	CHN	25.32	110.30	19.1	454.7	441.7	441.3	2.9	3.0	93	97	94
Xiamen	CHN	24.47	118.07	20.5	473.3	459.4	460.1	2.9	2.8	100	100	100
Saharanpur	IND	29.85	77.87	21.8	509.8	490.1	497.1	3.9	2.5	90	94	90
Heyuan	CHN	23.72	114.67	21.8	493.3	477.8	480.7	3.1	2.6	100	100	100
Taipei	TWN	25.07	121.55	22.8	507.7	491.0	495.0	3.3	2.5	100	100	100
Region type: Hot, annual average temperature from 23ºC to 28ºC*												
Hong Kong	CHN	22.32	114.17	23.1	506.7	491.5	494.8	3.0	2.4	100	100	100
New Delhi	IND	28.57	77.18	24.7	555.0	528.2	541.9	4.8	2.4	100	100	100
Patna	IND	25.27	85.17	25.2	555.4	531.9	544.1	4.2	2.0	100	100	100
Jaipur	IND	26.82	75.80	25.6	572.1	542.9	559.2	5.1	2.2	100	100	100
Nagpur	IND	21.10	79.05	26.8	589.7	559.7	578.2	5.1	1.9	100	100	100
Bangkok	THA	13.92	100.58	28.5	599.8	575.5	592.3	4.1	1.3	100	100	100

*Region type classifications adapted from the Thermal Universal Scale according to annual average temperature. This classification does not group regions according to climate conditions, it is used as only as a representative classification for this work.